Directional Emphasis Filtering in Artifact Metrics for Rejecting Raster-Scanning-Created Clones

Akira Iwahashi *, Naoki Yoshida , Tsutomu Matsumoto

Posted Date: 28 December 2023

doi: 10.20944/preprints202312.2194.v1

Keywords: Artifact metrics; Clone resistance; Frequency filtering; Raster scanning; Copy detection; Counterfeit

Article

Directional Emphasis Filtering in Artifact Metrics for Rejecting Raster-Scanning-Created Clones

Akira Iwahashi *, Naoki Yoshida and Tsutomu Matsumoto

Faculty of Environment and Information Studies, Yokohama National University in 79-7 Tokiwadai Hodogaya-ku, Yokohama-shi, Kanagawa-ken 240-0067 Japan ; ses.daigakuin-env@ynu.ac.jp

* Correspondence: iwahashi-akira-xp@ynu.jp

Abstract: Artifact metrics is a technology for authenticating artifacts based on their unique characteristics. The artifact-metric system offers "clone resistance," i.e., it makes it highly improbable to create another object exhibiting the same measured values as a genuine artifact. However, determined adversaries may still attempt to create imitations or clones with close physical characteristics to those of registered products, even if they cannot perfectly replicate the genuine product. Such clones serve to deceive users into believing they are genuine rather than counterfeits. Thus, in this study, we consider a scenario in which we measure raster-scanning-generated clones via a non-raster scanning method. Further, we employ image processing techniques to generate image data representing the clones and theoretically assess the filtering effects on these images. Our findings reveal that applying filters to specific frequency components in the spatial frequency domain can effectively highlight differences between raster-scanning-created clones and the corresponding genuine artifacts. Thus, we demonstrate directional emphasis filtering in artifact metrics as an effective approach for rejecting raster-scanning-created clones.

Keywords: artifact metrics; clone resistance; frequency filtering; raster scanning; copy detection; counterfeit

1. Introduction

In recent years, companies have emphasized the criticality of strengthening their supply chains in response to the impact of globalization. Further, to identify counterfeit, or inferior products, management methods for controlling individual products are desired. Thus, the utilization of "artifact metrics," a technology that exploits the physical characteristics of genuine individual products to control them, is gaining increased attention. Artifact metrics exploit the randomly generated physical characteristics of an artifact to authenticate such an artifact. Furthermore, as it exploits the physical characteristics of a unique product, it ensures the management of such a product without requiring tags, etc. Additionally, the international standardization of their application is also underway[1].

Assuming a malicious adversary creates a fitting counterfeit, companies can employ the artifact-metric system to identify and remove it from the market by exploiting the fact that the physical characteristics of the counterfeit are not registered. However, a more sophisticated attacker may create a counterfeit whose physical characteristics are as close as possible to those of the already registered product and pass it off as the genuine product ;such a counterfeit is called a clone. To be prepared against such adversaries, the artifact-metric system must be sufficiently clone-resistant, i.e., capable of rejecting clones.

The existing mainstream artifact-metrics systems include those that employ optical cameras to measure microscopic physical features[2][3]. When artifact metrics are based on microscopic features, attackers can create precise clones via various methods, such as raster processing, or stacking. Owing to the employed creation method, the clone may closely resemble the original in one axis, and fail to in another axis. Thus, based on these clone characteristics, the artifact-metric system may be capable of rejecting clones during matching using a spatial-frequency filter.

Preprints (www.preprints.org) | NOT PEER-REVIEWED | Posted: 28 December 2023 doi:10.20944/preprints202312.2194.v1

Based on the foregoing theory, we assumed a cloning scenario, generated image-processing-based image data, and theoretically demonstrated the effect of spatial frequency filtering on clone resistance. The results indicate that frequency filtering along specific directions in the spatial-frequency domain improves the clone-resistance of the artifact-metric system. We confirm that directional emphasis filtering is an effective artifact-metric strategy for rejecting raster-scanning-created clones.

2. Artifact Metrics

2.1. Properties of Artifact Metrics

The measured values (information) of the physical features (artifact-metric elements) comprising artifact metrics are determined by the object of interest and artifact-metric system (measurement system).

Artifact metrics require the following four properties

Individuality

Individuality refers to the properties that are unique for individual objects.

Read stability

Read stability refers to the properties whose values can be stably measured from individual objects.

Durability

Durability refers to the possibility of measuring stable values that are equivalent to those at the time of registration from individual objects that have changed or deteriorated over time.

Clone resistance

Clone resistance refers to the near impossibility of reproducing a clone with equivalent values to those of the original individual.

2.2. Configuration of the Artifact-Metric System

An artifact-metric system comprises the following processes: "measurement," where the artifact metric elements are captured by a measuring instrument; "data generation," where the captured image data are corrected and cropped to generate data for matching; "registration," where the generated data are used as templates and stored in a database; and "matching," where the similarity between the generated and matching data is calculated and authenticated. The general flow is shown below.

It consists of two phases: the registration (storing the registration data in the database) and authentication (matching against the stored data and outputting the decision results) phases (Figure 1).

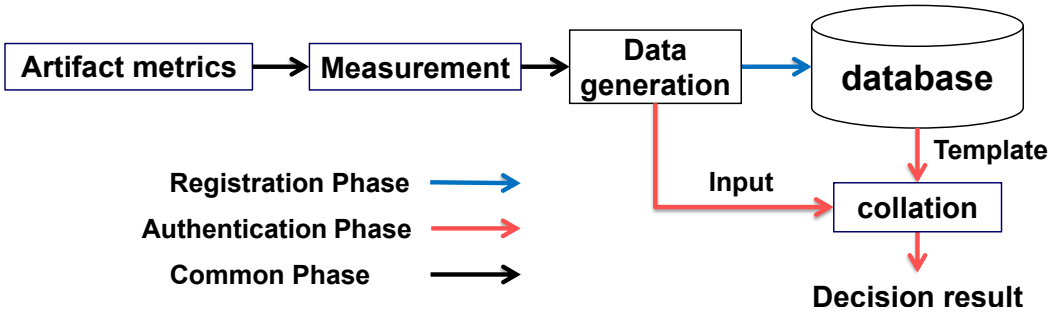

Figure 1. Artifact-metric system flow.

Preprints (www.preprints.org) | NOT PEER-REVIEWED | Posted: 28 December 2023 doi:10.20944/preprints202312.2194.v1

I **Registration Phase**

1. The artifact metric element p is measured with a measurement sensor to obtain a unique pattern.
2. The data T_p used for matching is generated from the unique patterns.
3. T_p is registered as template data.

II **Authentication Phase**

1. p is measured with a sensor to obtain a unique pattern.
2. The data I_p used for matching is generated from the unique patterns.
3. I_p is matched against T_p and accepted or rejected if the similarity is above or below a threshold, respectively.

2.3. Evaluation of Artifact-Metric Systems

The four properties discussed in the previous are required for the determination of the feasibility of an artifact feature as an artifact-metric element.

Indicators for evaluating artifact metric systems are defined in ISO22387[1]. The evaluation indicators are as follows (Figure 2):

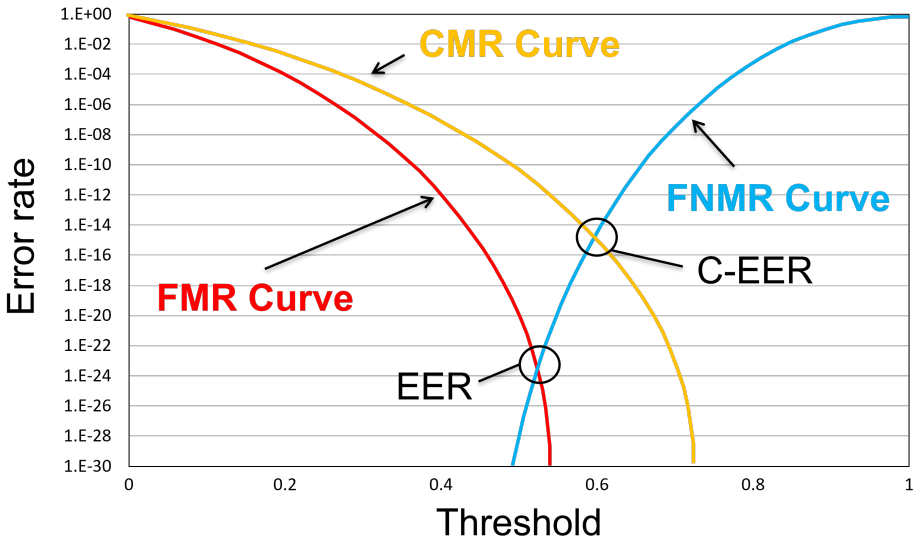

Figure 2. FMR, FNMR, CMR curves and EER.

False Non-Match Rate

False non-match rate (FNMR) refers to the probability of erroneously judging that artifacts are in disagreement when they agree.

False Match Rate

False match rate (FMR) is the probability of erroneously judging an artifact as a match when it is a mismatch.

Clone Match Rate

Clone match rate (CMR) is the probability of erroneously judging a clone as a match when it is a mismatch.

Equal Error Rate

Equal error rate (EER) is an error rate (ER) at which FMR and FNMR are equal.

Clone Equal Error Rate

Clone Equal Error Rate (c-EER) is an error rate (ER) at which CMR and FNMR are equal.

 doi:10.20944/preprints202312.2194.v1

The threshold corresponding to EER is often used to set the decision threshold during pattern matching, and EER is used as a representative measure of authentication accuracy when comparing matching algorithms. Further, CMR is used as a security evaluation index for cloning. As CMR varies with the matching algorithm, the security rating for clones is crucial. However, depending on the number of experimental data, EER and C-EER are not always obtained. Therefore, in this experiment, the C-F gap was used as a tentative index to compare the accuracy from the obtained FNMR and CMR curves for evaluation. The definition of the C-F gap is given below.

C-F gap

The difference between the maximum similarity in CMR and the minimum similarity in FNMR when the CMR and FNMR curves do not intersect is the C–F gap. It varies with ER, so ERs must be consistent when comparing accuracies.

3. Mainstream Cloning Methods and the Proposed Method

The following measurement and printing methods were assumed in this study:

Raster scanning

This method comprises measuring or printing one line (row) of data at a time to process a surface, followed by repeating the process.

Full scanning

Full scanning is a method for measuring or printing the entire object in one step.

Here, we considered a scenario in which an attacker creates a clone using "Raster scanning" against an artifact-metric system that uses image data obtained by creating and measuring artifacts using "Full scanning". We examine the effective image-processing method for this scenario.

3.1. Cloning Methods

Reference [4] provides a classification of clones in the artifact metric system, and they can be broadly divided into two: clones that are not aimed at reproducing the physical structure of the original object and those that are aimed at reproducing it.

Cloning, which is not aimed at reproducing the physical structure, is an attack method that exploits vulnerabilities regarding how an artifact-metric system is constructed or tuned. It comprises replay, wolf, and simulated attacks.

Cloning that is aimed at reproducing the physical structure will always be judged as a match by the system if it can be reproduced exactly. Such a cloning attack is called a hardcopy attack. If this attack is assumed for an artifact metric element whose identity is the fine three-dimensional (3D) shape of the surface of the object, the clones that are produced by "Raster scanning" methods, such as 3D printing, or charged-particle-beam processing lithography, can imitate the original with high accuracy, thus posing a significant threat.

3.2. Differences with the Original Object Based on "Raster Scanning"

The "Raster scanning"-based imaging process scans in one direction (x-direction) for each horizontal resolution and moves in the perpendicular direction (y-direction) for that resolution. At this time, a 3D pattern of any size is drawn in the z direction (perpendicular to the x and y directions) for each resolution in the x and y directions. In devices that draw fine 3D patterns using "Raster scanning", the pattern is formed by moving the imaging device, such as a laser, or probe, closer to, or farther from the object to be drawn by voltage or thermal control or both. In the case of fine and random patterns, voltage control is very challenging, complicating the high-accuracy mimicking of the pattern. Similarly, thermal control may leave residual heat when switching from high to low temperatures, and the needle tip may not warm up sufficiently when switching from low to high temperatures. Therefore,

Preprints (www.preprints.org) | NOT PEER-REVIEWED | Posted: 28 December 2023 doi:10.20944/preprints202312.2194.v1

when cloning via "Raster scanning," a few differences would exist between the clone and the original because of such errors.

Based on the foregoing, the difference between the clones created by “Raster scanning“ and “Full scanning“ is evident at two points.

1. Different z-directional offsets per horizontal resolution in the y-direction
2. Different x-directional offsets per horizontal resolution in the y-direction

Based on these assumed differences, it is assumable that the imitation accuracy will be reduced by the numerous differences for a specific direction. Put differently, using the frequency components in a specific direction as a factor for matching may represent an effective strategy for clone refection. Therefore, we examined the possibility of rejecting a clone based on the differences between the "Raster scanning"-obtained clone and “Full scanning“-obtained original by applying spatial frequency filtering to emphasize the frequency components in a specific direction using the generated image data assuming the clone was created via image processing.

3.3. Proposed Method

We propose directional emphasis filtering as the spatial frequency filtering to highlight the differences between the "Raster scanning"-and “Full scanning“-obtained clone and original, respectively.

Assuming G is the output of applying the frequency filter, H, to the matrix, F, in which the first and third quadrants and the second and fourth quadrants are swapped after the Fourier transform, the frequency filtering will be represented by the following equation.

$$G = F \odot H.$$

Our proposed spatial frequency filtering emphasizes the number of frequency component distributions in an arbitrary region with a constant coefficient. Assuming the pixel value of the to-be-filtered image is $F(i,j)$, the width is w, and the height is h, Each filter, $H(i,j)$, of the proposed method will be given by

Non-Horizontal and Vertical Emphasis Filter (N-HVEF):

$$H(i,j) = \begin{cases} k & |i - \frac{w}{2}| > \frac{r}{2} \; and \; |j - \frac{h}{2}| > \frac{r}{2} \\ 1 & \text{otherwise} \end{cases}$$

Non-Vertical Emphasis Filter (N-VEF):

$$H(i,j) = \begin{cases} k & |j - \frac{h}{2}| > \frac{r}{2} \\ 1 & \text{otherwise} \end{cases}$$

Non-Horizontal Emphasis Filter (N-HEF):

$$H(i,j) = \begin{cases} k & |i - \frac{w}{2}| > \frac{r}{2} \\ 1 & \text{otherwise} \end{cases},$$

where k is the number of times the frequency distribution of a region is emphasized and r is the width of the region, each of which is an arbitrary constant that is greater than or equal to 1. Each filter is illustrated in Figure 3. The pixel values in the areas filled with black remain the same, whereas the pixel values in the other areas are emphasized by a factor, k.

Preprints (www.preprints.org) | NOT PEER-REVIEWED | Posted: 28 December 2023 doi:10.20944/preprints202312.2194.v1

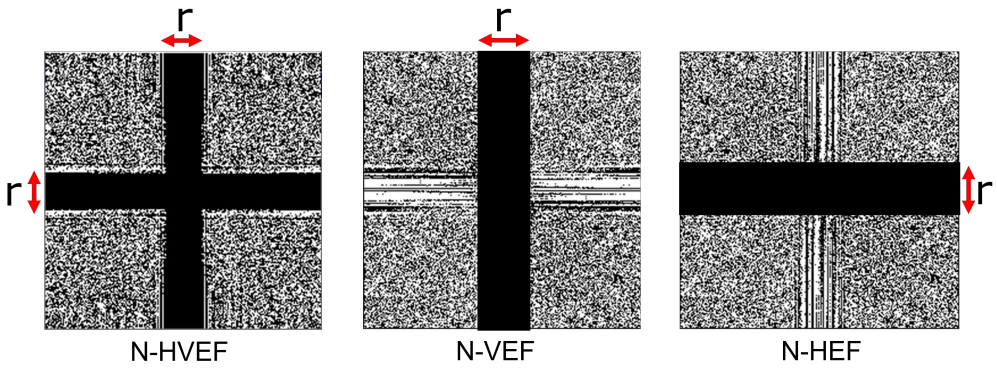

Figure 3. Filters of the proposed method.

4. Experiments to Evaluate the Effectiveness of Filtering

In this section, we evaluated whether the spatial frequency filtering of the proposed method is effective for rejecting “Raster scanning”-created clones, and the experimental procedure is presented below. Except otherwise specified, the term “clone” refers to clones created via "Raster scanning" hereafter.

1. Create simulated images of the data from which the original and clone were measured.
2. Calculate the similarity between the original and clone data using the correlation coefficient.
3. Apply filtering to the simulated image data created.
4. Calculate the similarity between the filtered original and filtered clone data using the correlation coefficient.
5. Evaluate the effect of filtering by comparing the results of Steps 2 and 4.

4.1. Image Processing for Generating the Image Data

To measure artifacts via "full scanning", measurement errors such as brightness, and focus shifts occur with each measurement. Brightness shift is simulated by adding an arbitrary constant to the pixel values in the image, and the focus shift is simulated by smoothening. The process of simulating measurement errors comprises the following:

Brightness shift

Add 5 to all the elements in the image. However, if the pixel value is greater than 255, set the pixel value to 255.

Focus shift

Smoothen to the image with a 2*2 normalized box filter using the openCV.blur function in Python.

Next, we consider an image processing method for simulating the differences in a clone, as described in Section III-B. The offsets in the x-direction, which differ from one horizontal resolution to another in the y-direction, are called "Row misalignment," and the offsets in the z-direction, which differ from one horizontal resolution to another in the y-direction, are referred to as "Height misalignment." These misalignments are simulated by the following image processing (Figure 4).

Preprints (www.preprints.org) | NOT PEER-REVIEWED | Posted: 28 December 2023 doi:10.20944/preprints202312.2194.v1

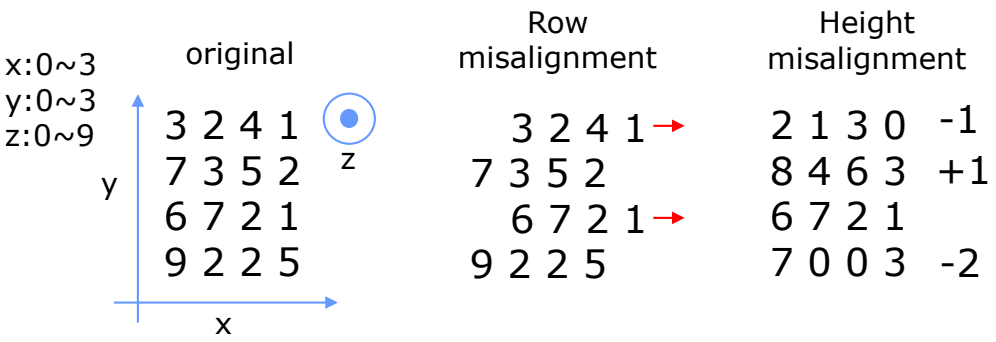

Figure 4. Processes that assume misalignment caused by raster scanning.

Row Misalignment

In each row of the image matrix, the process is performed randomly from the following: 1. shift by one element to the left, 2. shift by one element to the right, and 3. do nothing. The blank elements due to shifting elements are filled with zeros.

Height Misalignment

In each row of the matrix, randomly determine an integer, a, from an arbitrarily set range (-5 to 5) and add it to all the elements in that row. If the pixel value is less than 0, it is assumed to be 0: if it is greater than 255, it is assumed to be 255.

4.2. Experimental Generation of the Image Data

In this experiment, we selected twenty six images (Figure 5) provided in the USC-SIPI image database[5]. By experimenting with these images, we could verify the robustness of the proposed method with respect to frequency.

The selected image is a grayscale image in three different sizes, 256px × 256px , 512px × 512px and 1024px × 1024px, and is considered the original image.

Next, the brightness, and focus shifts described previously are applied to the original image, which is used as data for calculating FNMR (referred to as the FNMR data).

Subsequently, The FNMR data are used to generate data for calculating CMR (referred to as the CMR data), assuming the clone. The application of row or height misalignment or both to the FNMR data generates the CMR data (Figure 6).

Figure 5. Image data targeted in the experiment.

Preprints (www.preprints.org) | NOT PEER-REVIEWED | Posted: 28 December 2023 doi:10.20944/preprints202312.2194.v1

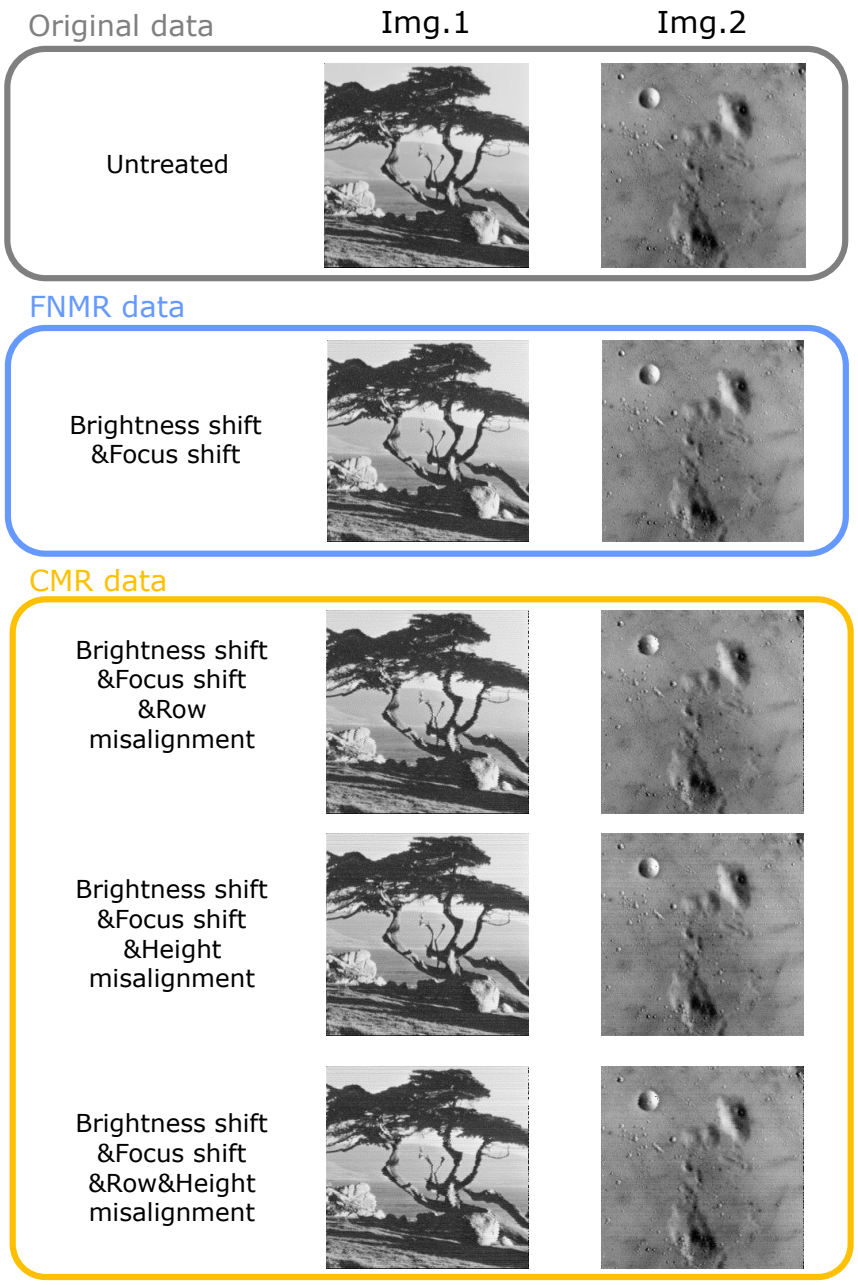

Figure 6. FNMR and CMR data.

4.3. Collation Method

In the pattern-matching process, the similarity between both images is calculated, and the acceptance, or rejection is determined based on the magnitude of the similarity. In this experiment, we used one of Pearson's correlation coefficients, a statistic called the "Zero Mean Normalized Cross-Correlation (ZNCC) to calculate the similarity. ZNCC does not change even if the mean pixel values of both image areas being compared differ. Therefore, it is robust to illumination changes.

Let the pixel value of the input image be $I(i, j)$, the pixel value of the template image be $T(i, j)$, the width of the template image be w, and height be h, the ZNCC value is calculated by the following equation:

Preprints (www.preprints.org) | NOT PEER-REVIEWED | Posted: 28 December 2023 doi:10.20944/preprints202312.2194.v1

$$ZNCC = \frac{\sum_{j=0}^{h-1}\sum_{i=0}^{w-1}(I(i,j)-\bar{I})(T(i,j)-\bar{T})}{\sqrt{\sum_{j=0}^{h-1}\sum_{i=0}^{w-1}(I(i,j)-\bar{I})^2\sum_{j=0}^{h-1}\sum_{i=0}^{w-1}(T(i,j)-\bar{T})^2}}$$

The value of ZNCC ranges from -1 to +1. The higher the absolute value, the more the correlation between the two images. However, as no two images correlate negatively in this experimental image matching, the closer the value is to +1, the more similar the two images are.

We implemented pattern matching using the cv2.match Template of OpenCV. This function takes an input image and a template one as arguments. The output of the function is the ZNCC values of all the candidates while shifting the input and template images horizontally and vertically, respectively. The highest value is taken as the similarity. In this experiment, the input images were smaller than the template image by 10 px in height and width.

4.4. Experimental Results

For each original image, the similarity was calculated by matching the image from the original to the FNMR data and by matching the original to each of the three CMR data. We experimented with various pairs of filter parameters, (r,k), and observed that the parameter with the widest C-F gap for both misalignments was (r=w*0.2, k=20). The results are presented in Table 1.

Table 1. Degree of similarity in each matching (zncc).

Template	Input image			
	FNMR	CMR		
	-	Row	Height	Both
Tree	0.997740	0.984970	0.996646	0.984862
Aerial	0.995329	0.953731	0.992772	0.953694
Clock	0.998111	0.985054	0.996652	0.984543
Girl2	0.998924	0.985869	0.996641	0.983194
House1	0.998924	0.988524	0.996647	0.986241
Jelly beans	0.999698	0.990281	0.996120	0.986455
Moon surface	0.990674	0.956606	0.984495	0.951811
Resolution chart	0.995162	0.944530	0.994940	0.938721
Aerial2	0.995115	0.955345	0.991834	0.948079
APC	0.993205	0.980802	0.984179	0.971939
barbara512	0.996189	0.950449	0.994583	0.948784
Car and APCs	0.997519	0.988071	0.992836	0.983725
Car and APCs2	0.996560	0.983755	0.989817	0.976854
Fishing Boat	0.996647	0.971964	0.994345	0.971366
Girl(Elaine)	0.996163	0.989592	0.993933	0.987271
Girl(tiffany)	0.994574	0.971821	0.988053	0.967310
Pixel ruler	0.949280	0.746146	0.950330	0.740673
Stream and bridge	0.993764	0.973471	0.992022	0.971811
Tank	0.993473	0.974026	0.986598	0.969028
Tank2	0.986849	0.950078	0.978364	0.939182
Tank3	0.995079	0.983840	0.991151	0.980002
Truck and APCs	0.992350	0.974347	0.988119	0.969204
Truck and APCs2	0.992088	0.972477	0.987535	0.967563
Truck	0.995300	0.980922	0.988553	0.975057
Airport	0.989911	0.955410	0.986027	0.951934
Man	0.998665	0.989175	0.997095	0.987876

In unfiltered matching, the C-F gap was less than 0.05 for all matches except "Resolution chart" and "Pixel ruler". Given these C-F gaps, it is highly likely that clones would be accepted as originals even if the “Raster scanning”-based differences existed therein. Figures 7–9 shows the results of the calculation of the C-F gap from the similarity.

Preprints (www.preprints.org) | NOT PEER-REVIEWED | Posted: 28 December 2023 doi:10.20944/preprints202312.2194.v1

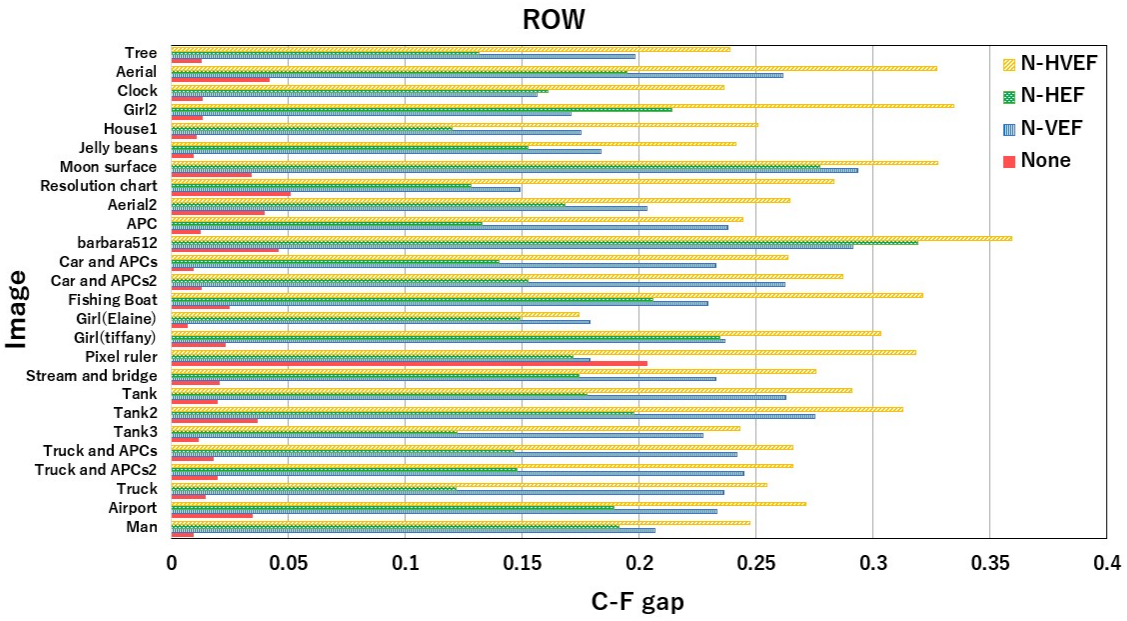

Figure 7. C-F gap in row misalignment.

Regarding row misalignment, the most effective filter was N-HVEF, which widened the C-F gap by up to a factor of 27.8 after applying N-HVEF compared with the unfiltered C-F gap. This is because the clone with row misalignment could mimic the horizontal and vertical components of the spatial–frequency domain, as well as comprises more differences in the diagonal components.

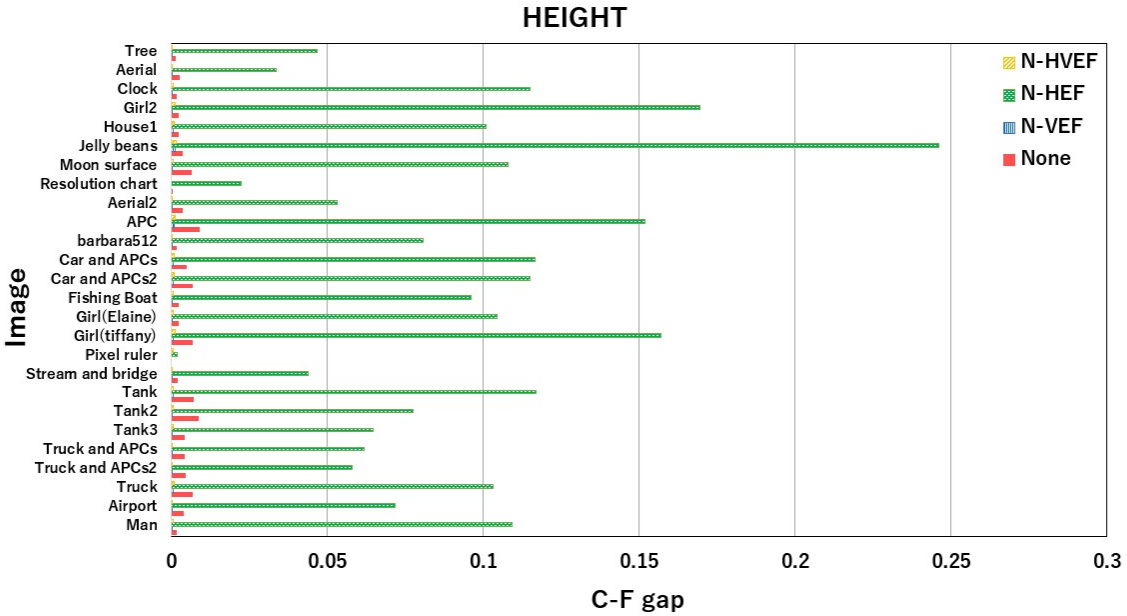

Figure 8. C-F gap in height misalignment.

Regarding the height misalignment, N-VEF, and N-HVEF did not exert a significant effect, except N-HEF, where the C-F gap widened by up to a factor of 100.3 compared with the unfiltered case. This is because the clones exhibiting height misalignment displayed an evident difference in the vertical component of the spatial–frequency domain.

Preprints (www.preprints.org) | NOT PEER-REVIEWED | Posted: 28 December 2023 doi:10.20944/preprints202312.2194.v1

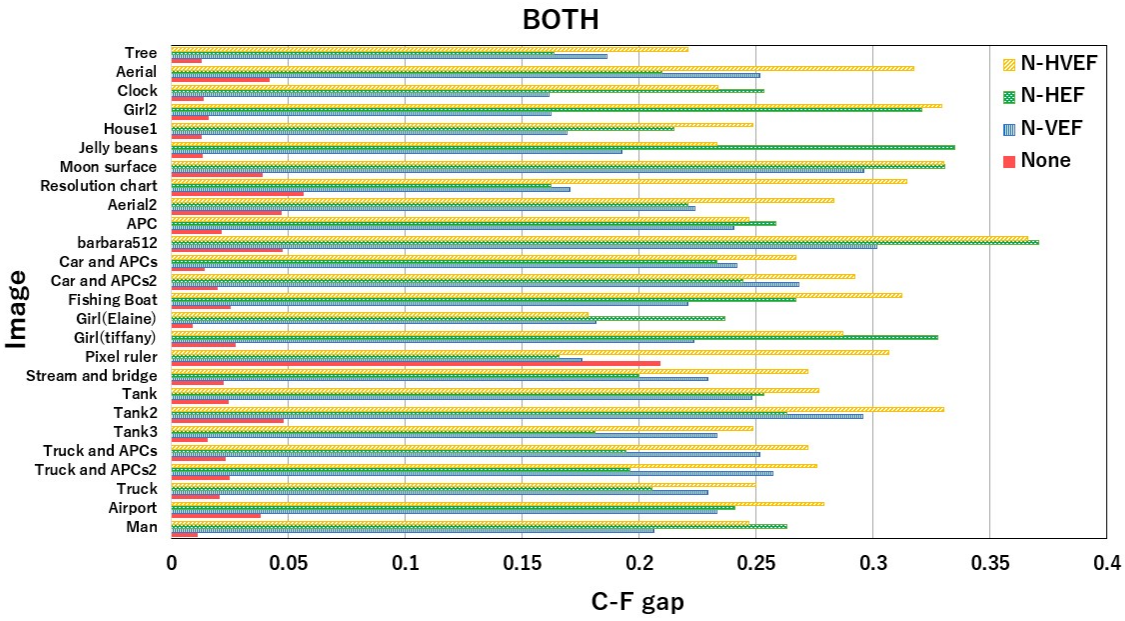

Figure 9. C-F gap in row and height misalignment.

Finally, considering the results including both misalignments, the clone–rejection accuracy improved with all the filters. The optimal filter depended on the image, but N-HVEF or N-HEF effective, widening the C-F gap by a factor of 22-25 compared to no filter.

Regarding the row misalignment, the results indicate that N-HVEF, which emphasizes spatial–frequency components other than those in the horizontal and vertical directions (x– and y–directions), which are the axes of operating raster scanning, is effective for clone rejection. However, regarding both misalignments, the filters emphasizing components other than those in the raster–scanning direction (x–direction) are effective. Conversely, regarding clones with only height misalignment, a filter based on the order of movement in the raster–scanning direction is necessary.

A comparison of the untreated image (man.bmp) with the most C-F gap extension in the experiment for both misalignments, and the image with N-HVEF and N-HEF applied to the image containing both misalignments (man.bmp) is shown in Figure 10.

Compared to the unprocessed image, both filters show a more pronounced noise in the horizontal direction and an enhancement of the difference from the original. Furthermore, N-HEF emphasises horizontal features more than N-HVEF, and N-HEF seems to be more effective for images containing both types of displacement. On the other hand, for real-world applications, it is unclear in which direction an attacker would clone, and filtering in one direction alone is not sufficient.Therefore, the system must be constructed by changing the combination based on the expected clones and needs, such as implementing N-VEF, followed by N-HEF, in an actual operation. Moreover, the clone resistance improved even after smoothening the clone. This indicates that our proposed method is effective even when the resolution of the artifact imaging instrument is lower than that of the cloning instrument.

Preprints (www.preprints.org) | NOT PEER-REVIEWED | Posted: 28 December 2023 doi:10.20944/preprints202312.2194.v1

Figure 10. Different filter effects based on the frequency of the image.

5. Summary and Future Outlook

By employing image processing to reproduce the assumed errors in raster–scanning–created clones, this study was conducted to investigate whether filtering along a specific directional component within the spatial frequency is effective for clone rejection.

The results reveal that the proposed filtering method can effectively improve clone resistance. Regarding row misalignment, N-HVEF was most effective for clone rejection. Regarding height misalignment, the filter that emphasized the spatial–frequency components other than a certain direction was the most effective for clone rejection.

To demonstrate that the theoretical experiments presented herein are valid for actual systems, we are currently exploring thermal scanning probe lithography to create clones that mimic nanometer-scale artifact metrics based on the resist collapse phenomenon[6][7]. The clones exhibit the expected row and height misalignments, and we will clarify whether they can be rejected by applying the spatial frequency filtering of the proposed method to the artifact metrics.

Author Contributions: Conceptualization,A.I. and N.Y.; methodology, A.I. and N.Y.; software, A.I.; validation, A.I.; formal analysis, A.I.; investigation, A.I.; resources, A.I; data curation, A.I.; writing—original draft preparation, A.I. and N.Y.; writing—review and editing, A.I. and N.Y. ; supervision, N.Y and T.M.; project administration, T.M.; funding acquisition, T.M. All authors have read and agreed to the published version of the manuscript.

Funding: A part of this paper is based on results obtained from a project, JPNP23013, commissioned by the New Energy and Industrial Technology Development Organization (NEDO).

Data Availability Statement: The data that support the findings of this study are openly available at [http://www.ess.ic.kanagawa-it.ac.jp/app_images_j.html], reference number [5].

Conflicts of Interest: The authors declare no conflict of interest.

 doi:10.20944/preprints202312.2194.v1

References

1. ISO. (2022). ISO 22387:2022(en) Security and resilience — Authenticity, integrity and trust for products and documents — Validation procedures for the application of artefact metrics [ISO 22387]. https://www.iso.org/standard/80717.html
2. T.Matsumoto, N.Yoshida, S.Nishio, M.Hoga, Y.Ohyagi, N.Tate, M.Naruse, "Optical nano artifact metrics using silicon random nanostructures," Scientific Reports, Vol.6, No.32438, Aug 2016.
3. Ken Takano, Atsushi Miyazaki, Mamoru Saito, Masaaki Sugimoto, Tadatomo Yamada, Shinya Takyu, "A New Authentication Method Using The Smart Individuality Printing to Improve The Traceability of Semiconductor Packages," International Conference on Electronics Packaging April 2023.
4. Y.Tamura, M.Une, "Towards a method for evaluating cloning resistance in artificial metric systems," Bank of Japan. Institute for Monetary and Economic Studies, IMES discussion paper series, 2009/7, 183-218 (2009)
5. Kanagawa Institute of Technology, "Signal Processing Application Laboratory," http://www.ess.ic.kanagawa-it.ac.jp/app_images_ j.html
6. T.Matsumoto, M.Hoga, Y.Ohyagi, M.Ishikawa, M.Naruse, K.Hanaki, R.Suzuki, D.Sekiguchi, N.Tate, M.Ohtsu, "Nano-artifact metrics based on random collapse of resist," Scientific Reports, Vol.4, No.6142, Aug 2014.
7. N.Yoshida, A.Iwahashi, M.Hoga, J.Ohta, K.Sumiya, T.Matsumoto, "Clone Resistance of Artifact Metrics: Scanning Probe Lithography Based Clones," IEICE Technical Report Hardware Security (HWS), HWS2022-88, Mar 2023.